

NOVEL SONOCHEMICAL SINGLE STEP FABRICATION OF NiO NANOPARTICLES

S. ATA^a, A. TABASSUM^a, M. I. DIN^{a*}, M. FATIMA^a, S. GHAFOR^a,
A. ISLAM^b, A. AHAD^c, M. A. BHATTI^d

^a*Institute of Chemistry, University of the Punjab, Lahore*

^b*Department of Polymer Engineering and Technology, University of the Punjab,
Lahore*

^c*Government Islamia College Civil Lines, Lahore*

^d*Mineral Processing Research Centre, PCSIR Laboratories Complex, Ferozpur
Road, Lahore*

A novel sonochemical route was reported for the manufacturing of nickel oxide (NiO) nanoparticles. The synthesized NiO nanoparticles were characterized by UV-visible spectroscopy, Fourier transform infrared (FTIR) spectroscopy, scanning electron microscopy (SEM), and energy dispersive X-Ray analysis (EDX). Their size calculated by SEM was ranges between 35 to 117 nm. The ability of NiO nanoparticles to remove lead ions from aqueous solutions was investigated. Several parameters such as dosage of the adsorbent, pH, shaking time and the effect of temperature were studied systematically and optimum values were chosen for subsequent isotherm modeling. Adsorption data obeyed both Langmuir and Freundlich isotherm models but fitted better with Langmuir isotherm model with highest uptake capacity of 166 mg/g. The kinetics of the adsorption process followed pseudo-second-order rate equation. Thermodynamics studies illustrated endothermic nature of the process and its feasibility. The experimental results depicted that the NiO nanoparticles can likely be employed as an adsorbent for removing heavy metal ions from water.

(Received November 17, 2015; Accepted January 11, 2016)

Keywords: NiO nanoparticles, Pb(II) removal, Adsorption, Water treatment, Sonochemical synthesis, NiO adsorbent

1. Introduction

With the rapid development of industrial activities, environmental pollution caused by heavy metals becomes a serious problem [1]. Heavy metals such as lead, copper, arsenic, antimony, mercury, manganese, chromium, and cadmium are significantly toxic to ecological systems and human beings [2] as heavy metals are not biodegradable and tend to accumulate in living organisms causing serious health hazards [3]. Among these heavy metals, Pb (II) is one of the most toxic heavy metal [4]. Lead is released into water system from such sources as mining or metallurgical processes, plumbing, phosphate fertilizer, metal plating, electrodes, cables, ceramics, lead storage batteries, oil refinery, building construction, leaded gasoline, pigments, lead based paints, ammunition, and alloy industries [5]. The drinking water is a major source of lead exposure for the world population [6]. Lead poisoning causes paralysis, anemia, coma, brain damage, skin and lung cancer, kidney dysfunctions, bone diseases, convulsion, and even death. Lead also adversely affects reproductive system of women [7]. The World Health Organization (WHO) set the maximum permissible limit of lead in drinking water as low as 10 µg/L [8]. The amount of lead in drinking water of Pakistan is found to be ≤ 50 µg/L which is in agreement with the amount of

* Corresponding Author: imrandin2007@gmail.com

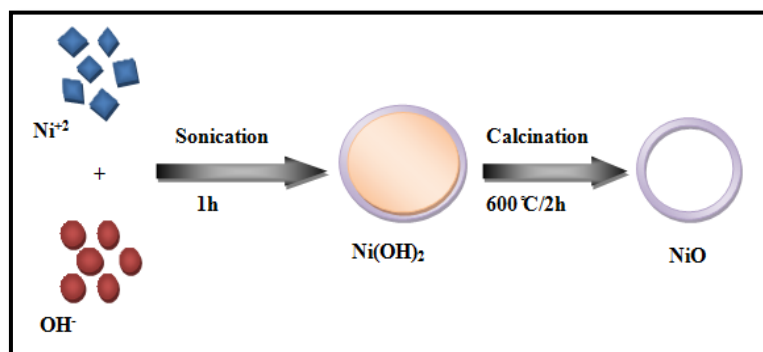
lead founds in most Asian countries. Therefore, effective removal of lead is necessary from water system to clean up the environment.

There are various techniques employed for the removal of lead such as ion exchange, chemical precipitation, floatation, coagulation, electrochemical treatment, evaporation, reverse osmosis, solvent extraction, membrane filtration and adsorption [9] however each process has its own applications and some limitations. Among these methods adsorption is one of the most promising and frequently used techniques due to its simplicity, low cost and high efficiency [10]. A large number of sorbents such as carbon materials, oxides and clay minerals have been employed for the removal of lead from aqueous system. But these sorbents either showed poor removal efficiencies or high cost. Hence there is a need for better and alternative sorbents which give maximum removal efficiency even at low concentrations for the removal of lead from water [11].

With the development of nanotechnology in recent years, nanoparticles due to their to unique chemical and physical properties such as large surface areas to volume ratio, fast adsorption rate, and high adsorption capacity, have shown their tremendous potential for the capture of inorganic and organic pollutants in water. A large number of nanoparticles have been studied for the removal of lead from water and proven to be promising adsorbents for environmental remediation [12].

Several methods such as hydrothermal, sol-gel, metal evaporation, electrochemical methods, and spray pyrolysis, have been developed to produce nanoparticles. Recently, the sonochemical methods have been acknowledged as a promising route for the preparation of variety of nanoparticles as it based on that when ultrasonic waves passes through a liquid medium, a large number of micro bubbles form, grow, and collapse in very short time, a process called as cavitation. The collapse of micro bubbles generates instantaneous temperatures of several thousand degrees ($>5000\text{ }^{\circ}\text{C}$) and pressure of several hundred atmospheres ($>500\text{atm}$) that can induce many changes in the morphology of nanoparticles during their preparation [13].

In this work novel sonochemical method was used for the fabrication of NiO nanoparticles. The as synthesized nanoparticles were evaluated as adsorbent for removal of Pb (II) ions from aqueous solutions. NiO nanoparticles, due to their quantum size and surface effects exhibit catalytic, electronic, optical, and magnetic properties that are significantly different than those of bulk-sized NiO [14]. Thus NiO nanoparticles have been chosen because of their low cost, high efficiency, small size, and also their small amount was used for adsorption experiments. The effect of pH, contact time, temperature and concentration of metal ion were examined systematically. Adsorption isotherms, kinetics and thermodynamics were also analyzed to evaluate adsorption mechanism



Scheme 1. Graphical abstract of NiO synthesis

2. Experimental

Chemicals and reagents

Nickel sulfate ($\text{NiSO}_4 \cdot 6\text{H}_2\text{O}$), sodium hydroxide (NaOH), cetyl trimethylammonium bromide (CTAB), nitric acid (HNO_3), lead Nitrate ($\text{Pb}(\text{NO}_3)_2$), were of analytical grade with 99.9% purity, obtained from Merck Germany and were used as received without further purification. Stock solution (1000mg/L) of $\text{Pb}(\text{NO}_3)_2$ was prepared by dissolving stoichiometric amount in 1% HNO_3 to prevent hydrolysis and further diluted with distilled water. The stock solution was further diluted to obtain working solutions of varying concentrations for next experiments.

Preparation of NiO nanoparticles

NiO nanoparticles were prepared via sonochemical method in the presence of cetyl trimethylammonium bromide (CTAB). A 100 mL of 0.2 M NaOH solution was added drop wise into 100 mL of 0.05 M $\text{NiSO}_4 \cdot 6\text{H}_2\text{O}$ solution containing 100 mg/L of cetyl trimethylammonium bromide (CTAB) under sonication condition for approximately 1h. The obtained green colored precipitates were separated by centrifugation at 3000 rpm for 20 min, washed thoroughly with distilled water and methanol upto $\text{pH}=7$, dried in hot air oven at 70°C overnight and finally calcined in air at 600°C for 2 h.

Characterization

UV-Visible spectroscopy was performed on T 90+ Double Beam UV-VIS Spectrophotometer (PG Instruments) in the wavelength range of 300-400nm. Fourier transform infrared spectrum (FTIR) was taken with Nicolet 6700 FT-IR spectrometer (Thermo Scientific) between 4000 and 400 cm^{-1} . The morphology, size and elemental composition was examined by JSM-6490LV scanning electron microscopy (SEM) coupled with an X-ray energy-dispersive spectrometer (EDS) at working voltage of 20kV. The pH measurements were made with HI5222-digital pH meter (Hanna Instruments). The concentration of metal ion was determined by A Analyst - 400 Flame Atomic Absorption Spectrometer (PerkinElmer) using an air-acetylene flame.

Adsorption Experiments

The adsorption experiments of Pb (II) ions on NiO nanoparticles were conducted in a batch method, which permits the complete evaluation of parameters that influences the process of adsorption. In this method, a series of 100 mL glass flasks were filled with 50 mL Pb (II) ion solution of varying concentrations (50-500 mg/L). Then equal amount (0.06 g) of NiO nanoparticles was added into each flask and subjected for agitation at 200 rpm until equilibrium was attained (30 min). The resultant solutions were centrifuged at 3000 rpm for 20 min and the supernatant liquids were subjected to the determination of Pb (II) ions using Atomic Absorption Spectrophotometer (AAS). All the experiments were conducted at room temperature ($293 \pm 1\text{ K}$), and the pH of the solution was maintained unaltered.

The metal ion removal efficiency (%) R was calculated by equation (1) and the amount of metal ion adsorbed at equilibrium, q_e (mg/g) was calculated by equation (2) as:

$$R (\%) = (C_o - C_e) \frac{100}{C_o} \quad (1)$$

$$q_e = (C_o - C_e) \frac{V}{W} \quad (2)$$

Where, C_o and C_e are the initial and equilibrium concentrations (mg/L) respectively, V is the volume of metal ion solution (L) and W is the amount of adsorbent used (g).

The effect of adsorbent dose was evaluated by varying amount of adsorbent as 0.02-0.20 g while keeping metal ion concentration constant (50 mg/L). The effect of pH on the extent of metal ion adsorption was studied by agitating 50 mL of 50 mg/L metal ion solution with 0.06 g of NiO for predetermined equilibrium time at pH ranging from 3.0-8.0 and all other experiments were conducted at pH 6 unless and otherwise mentioned. The pH of metal ion solution was adjusted by

using 0.1 M HNO₃ or 0.1 M NaOH. To study the effect of contact time (adsorption kinetics), a set of experiments was conducted in the range of 5–30 min and the effect of temperature on the adsorption capacity of metal ions on NiO was also evaluated at a range of temperatures from 293 to 323 K, for the above said concentration of metal ion.

3. Results and Discussion

Characterization of NiO Nanoparticles

UV-visible Spectroscopy

UV-visible spectrum of NiO nanoparticles dispersed in distilled water is shown in Figure 1. The spectrum revealed a profound absorption peak at a wavelength of 330 nm, which is assigned as band gap absorption of NiO [15].

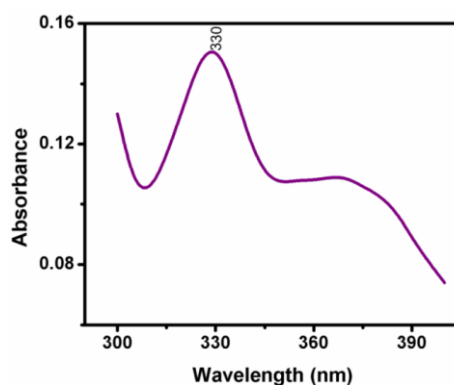


Fig. 1 UV-visible spectrum of NiO nanoparticles

The optical band gap energy (E_g) can be determined by using the following Tauc relationship:

$$\alpha h\nu^n = B (h\nu - E_g) \quad (3)$$

Where, α is the absorption coefficient, $h\nu$ is the energy of the incident photon, $n=1/2$ for direct band gap semiconductors, B is a constant, and E_g is the optical band gap energy [16]. The band gap energy of NiO nanoparticles can be calculated by extrapolation of linear portion of $(\alpha h\nu)^n$ versus $h\nu$ plot to energy axis as shown in Fig. 2. In this study, the band gap energy of NiO nanoparticles found to be 3.49eV and is in good agreement with the reported values in the range of 3.4 to 4.0eV [17]. Generally, semiconductors having nanoscale size show a blue shift in their absorption spectra. The shift of the absorption maximum towards short waves indicates an increase in the band gap. This can be explained as; when the size of the particle decreases to nanoscale, its absorption edge value move towards short wavelength as compared to bulk counterpart, and hence its band gap energy values increases, which are the evidences of the quantum confinement effect [18]. This trend is also in accordance with the as synthesized NiO thus confirming the formation of nanosized particles.

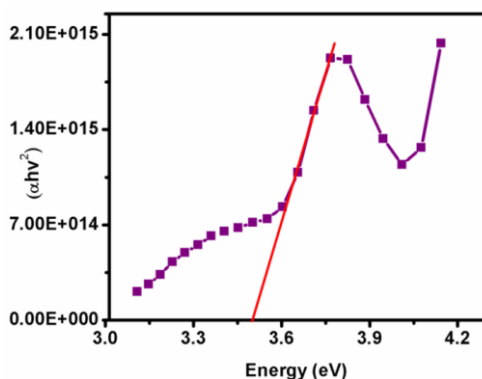


Fig. 2 Band gap values of NiO nanoparticles

Scanning electron microscopy

The scanning electron micrograph (SEM), exhibiting the morphology and size of the NiO nanoparticles synthesized by sonochemical method, at different magnifications are presented in Figure 3 (a,b). It is clear from the images that the nanoparticles have nearly spherical shape, and are of single phase with little agglomeration due to small size of particles and high surface energy. Their size ranges from 35 to 117 nm with some deviations. Figure 3 (c) shows EDX spectra of NiO, which clearly indicates the peak for the presence of nickel and oxygen as a major constituent of the synthesized NiO, with 98% percentage composition, and hence supporting the formation of NiO.

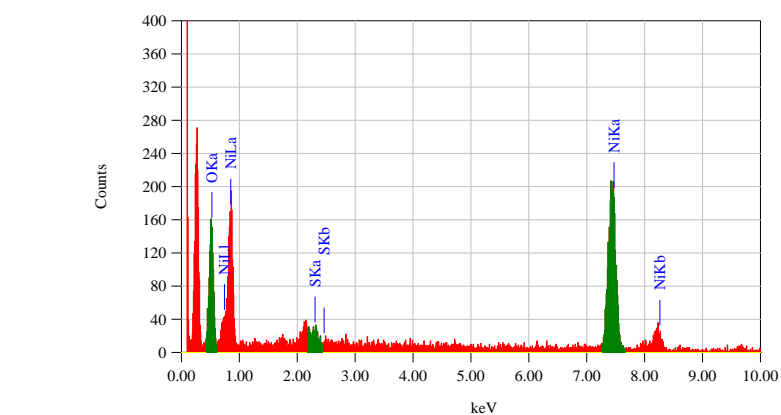
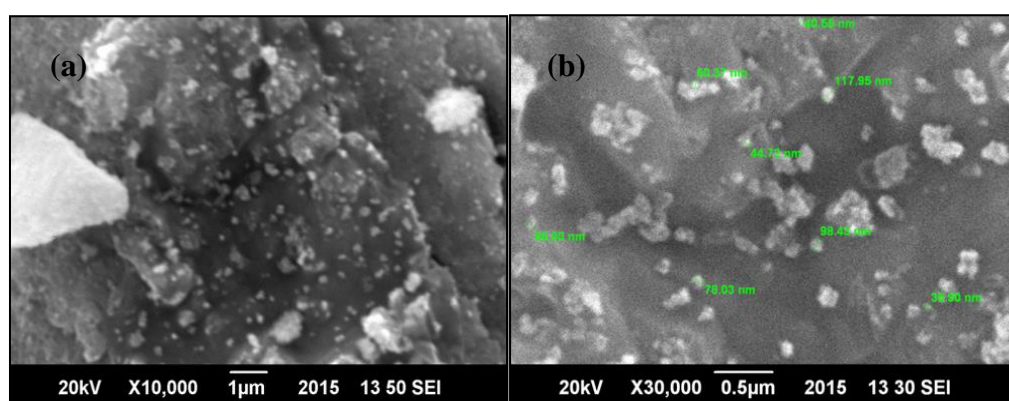


Fig. 3 SEM images of NiO nanoparticles at different magnifications (a) X10,000 (b) X30,000 (c) Energy dispersive X-Ray (EDX) spectrum of NiO nanoparticles

Fourier transform infrared spectroscopy

FTIR spectroscopy is generally used to understand the type and the nature of the functional groups. Inorganic metal oxides usually give absorption bands below 1000 cm^{-1} which arises due to their inter-atomic vibrations. FTIR spectrum of as synthesized NiO nanoparticles is shown in Figure 4. The peak at 3522 cm^{-1} is attributed to the stretching vibrational mode of hydroxyl group (O-H) and the peak at 1637 cm^{-1} is assigned to the bending vibrational mode of hydroxyl group (O-H). These peaks illustrated the presence of water molecules trapped on the surface of the particle from air. The distinct peak at 619 cm^{-1} is allocated to the stretching vibrational mode of Ni-O [18].

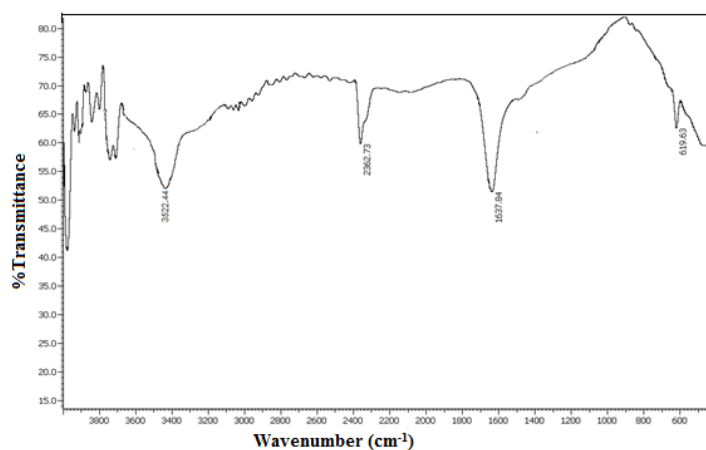


Fig. 4 FT-IR spectrum of NiO nanoparticles

Adsorption studies

Effect of adsorbent dose

The dose of adsorbent appeared to be an important parameter which effected the percentage removal of Pb (II) ions from aqueous solution. By increasing the dose of adsorbent from 0.02 to 0.06 g (Figure 5) the percentage adsorption reaches from 68 % (for 0.02 g) up to 100 % (for 0.06 g). The increase in the percentage adsorption may be attributed to the increase in available surface area which leads toward increase in the number of active sites available for adsorption [19]. But the further increase in the dose of adsorbent does not affect the percentage adsorption. This constancy in the adsorption may be due to the enrichment of adsorption sites [20] due to various types of interaction between adsorbed particles like aggregation, which increases the diffusional path length [21] and leads towards decrease in adsorption.

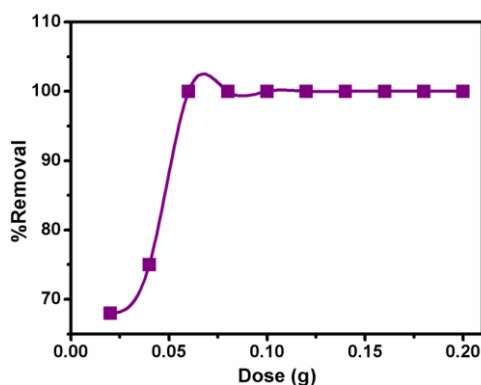


Fig. 5 Effect of dosage of adsorbent on percentage adsorption of Pb(II) by NiO

Effect of pH

The pH of the solution exerts profound influence on adsorption process of heavy metal ions because of its impact on the solubility of the metal ions, and the degree of ionization of the adsorbent [22]. Thus, adsorption should be conducted at optimum pH.

According to surface complex formation theory (SCF), the increase in pH leads to the decrease in the competition between metal ions and proton for the adsorption [23]. At low pH, in acidic region (<6), H^+ and Pb^{+2} species are prominent and compete for the same binding site thus lowers the percentage adsorption of metal ion. But at higher pH, the surface of NiO becomes negatively charged which favors interactions with metal ion and consequently enhances percent removal of metal ion. At pH range of 7-11, different species of Pb(II) like $Pb(OH)^+$ and $Pb(OH)_2$ becomes dominant which results in higher removal efficiency via adsorption of $Pb(OH)^+$ and precipitation of $Pb(OH)_2$ simultaneously [24]. Therefore, the effect of pH on the adsorption of Pb(II) onto NiO nanoparticles is carried out in the pH range of 3.0–8.0 with initial metal ion concentration of 50 mg/L at room temperature (293 ± 1 K).

The effect of pH of solution on adsorption process can be explained on the basis of surface charge of the adsorbent and the degree of speciation of adsorbates. At low pH, adsorbent behave as hydrous oxide (MOH) which is enclosed in pool of H^+ ions and changes to (MOH^{+2}) . At greater pH, hydroxyl ions react with hydrous oxide and converted it into deprotonated oxide (MO^-) which favors adsorption of metal cation. The reaction is described as [25];



Figure 6 exhibits the effect of pH of solution on the adsorption process of Pb (II) over NiO nanoparticles. At start, low pH values leads to lower percent removal of metal ion. But, with increasing pH, from 5-6, the percent removal efficiency goes towards higher values and reaches to a maximum (96%) at pH=6. After that precipitation of Pb (II) occurs as $Pb(OH)_2$ and therefore, optimum pH was chosen as 6. These results indicated that the pH of the solution had remarkable impact on the adsorption mechanism of Pb (II) on the NiO.

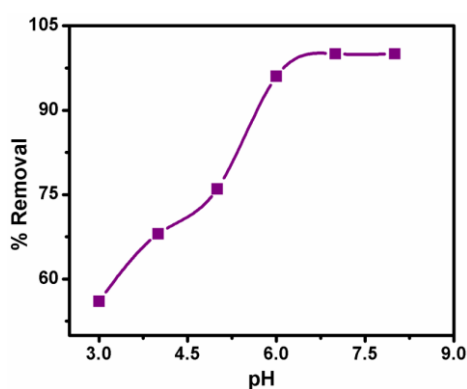


Fig. 6 Effect of initial solution pH on percentage adsorption of Pb (II) by NiO

Effect of contact time

Adsorption is generally a time reliance process. The influence of contact time on Pb (II) ions adsorption on NiO nanoparticles is studied in the range of 5–30 min at room temperature (293 ± 1 K) with initial metal ion concentration of 50 mg/L.

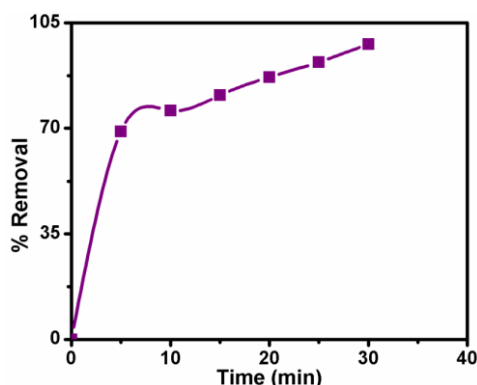


Fig. 7 Effect of contact time on percentage adsorption of Pb (II) by NiO

From Figure 7, it is obvious that the removal of metal ion enlarged with increasing shaking time until equilibrium attained. After reaching to equilibrium state, no prominent change in adsorption capacity is observed. This behavior is attributed to the saturation of active sites present on the surface of adsorbent. Further, the rate of adsorption is much faster at the start of process, which gradually slowed down and becomes constant at equilibrium point [26]. The experiments revealed that the equilibrium was reached within 30 min and hence this contact time is chosen for subsequent isotherm modeling.

Effect of initial metal ion concentration

The removal of Pb (II) ions by NiO nanoparticles as a function of their concentration is studied by varying the metal ion concentration from 50-500 mg/L at room temperature (293 ± 1 K) and pH=6, while keeping all other parameters constant. The reliance of the adsorption capacity of NiO on the equilibrium concentrations of Pb (II) ion is shown in Figure 8. The results revealed that on raising metal ion concentration, adsorption capacity (q_e) is also increased. This is illustrated as higher concentration offered large amount of metal ions at the solid/liquid interface, resulting in increased uptake of metal ions and hence provides maximum adsorption capacity.

But in contrast, increasing metal ion concentration leads to a decrease in percent removal of the metal ion. This can be explained as, lower concentration of metal ions in the solution make availability of less number of ions at the surface of adsorbent as compared to binding sites, thus results in highest percentage removal. However, with increasing concentration, large numbers of metal ions are found at solid surface and the numbers of sites become limited, which consequently lowers the percentage removal of the metal ion. This suggests that the removal of Pb (II) ions is highly concentration dependent [26].

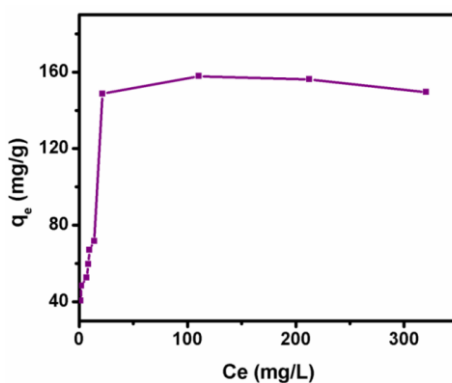


Fig. 8 Effect of equilibrium concentration on the adsorption capacity of Pb (II) NiO

Effect of temperature

The influence of temperature on Pb (II) ions adsorption onto NiO nanoparticles is carried out under varying temperatures ranging from 293 to 323 K with initial metal ion concentration of 50 mg/L at pH=6. Figure 9, demonstrated that the rise in temperature results in higher percentage removal of metal ion. This is illustrated as; the increase in temperature actually causes an enhancement in metal ions mobility and binding sites activity. This increased mobility of metal ions thus makes their effective collision with active solid phase and resulted in maximum percentage adsorption efficiency [26]. The increase in percentage adsorption with increasing temperature reflects endothermic nature of the process.

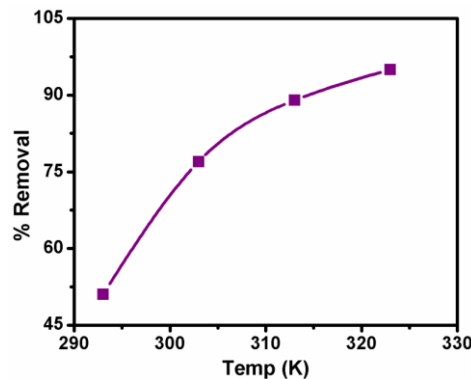


Fig. 9 Effect of temperature on percent adsorption of Pb (II) on NiO.

Modeling of adsorption isotherms

Adsorption isotherm is an equilibrium relation between the amount of metal ion adsorbed and the residual amount of metal ion in bulk solution, at a constant temperature. Adsorption isotherm demonstrated the actual interaction between sorbate and sorbent and thus helps in understanding the nature and mechanism of adsorption [27]. For a solid/liquid adsorption system, Langmuir and Freundlich models are the most employed models.

Langmuir isotherm model

Langmuir model postulates: (1) adsorption of molecules is a monolayer process; (2) all adsorption sites are alike and energetically equivalent; (3) each site can accommodate only one molecule or ion or atom; and (4) there is no chemical interaction between adsorbate and adsorbent [28-30].

The linear form of Langmuir model is given by following equation [31]:

$$\frac{C_e}{q_e} = \frac{C_e}{q_m} + \frac{1}{K_L q_m} \quad (7)$$

Where C_e is equilibrium concentration (mg/L) q_e is the amount of metals adsorbed at equilibrium (mg/g), q_m is the maximum adsorption capacity (mg/g), and k_L is the Langmuir equilibrium constant (L/mg) related to the adsorption energy coefficient. A plot of C_e/q_e versus C_e (Figure 10) would results in a straight line and the maximum adsorption capacity and bond energy of adsorbates can be calculated from the slope and intercept of that plot [32].

Essential characteristics of Langmuir isotherm can be expressed in terms of separation factor R_L , which is related to equilibrium constant by using the following relationship [32]:

$$R_L = \frac{1}{1 + K_L C_0} \quad (8)$$

Where, C_0 is the initial metal ion concentration (mg/L). The R_L value indicates the shape of isotherm; If $R_L > 1$ adsorption is unfavorable; if $R_L = 1$ it leads to linear isotherm formation; $R_L = 0$ adsorption is irreversible [33]. The R_L values calculated for Pb (II) ions are presented in Table 1. The R_L values are in a range of 0.150376-0.017391 for initial metal ion concentration of 50-500 mg/L and are greater than zero but less than one indicated that NiO is a suitable adsorbent for Pb (II) ions from aqueous solution.

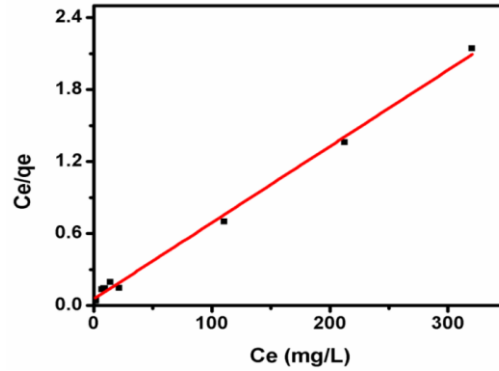


Fig. 10 Langmuir isotherm plot for the adsorption of Pb (II) ions onto NiO nanoparticles (adsorbent dosage 0.06 g, contact time 30 min; pH=6, temperature 293 K)

Table. 1 The separation factor (R_L) values for the adsorption of Pb (II) ions on NiO nanoparticles at pH=6 and 293 K

C_0	50	60	70	80	90	100	200	300	400	500
R_L	0.1503	0.12853	0.11223	0.09960	0.08952	0.08130	0.04237	0.02865	0.02164	0.01739

Freundlich isotherm model

The Freundlich isotherm model is an empirical model, which assumes multilayer sorption occur on a heterogeneous surface. The linear form of the Freundlich model is represented as [34];

$$\ln q_e = \ln K_f + \frac{1}{n} \ln C_e \quad (9)$$

Where, K_f and $1/n$ are Freundlich constants, K_f indicates the adsorption capacity and n is related to the adsorption energy distribution: if $n = 1$, adsorption is a linear process; if $n < 1$, adsorption is a chemical process; if $n > 1$, then adsorption is a physical process. The plot of $\ln q_e$ against $\ln C_e$ (Figure 11) should be a straight line with slope equal to $1/n$ and intercept equal to $\ln K_f$ [35].

The Langmuir and Freundlich parameters calculated from the slope and intercept of the isotherm plots are exhibited in Table 2. It is concluded from the data, that the experimental results fitted well into Langmuir isotherm model with high regression co-efficient of 0.9957 as compared to Freundlich isotherm model, thereby indicating monolayer and uniform adsorption of Pb (II) ions on NiO nanoparticles. The maximum uptake capacity of Pb (II) ions calculated by Langmuir isotherm plot is found to be 166 mg/g.

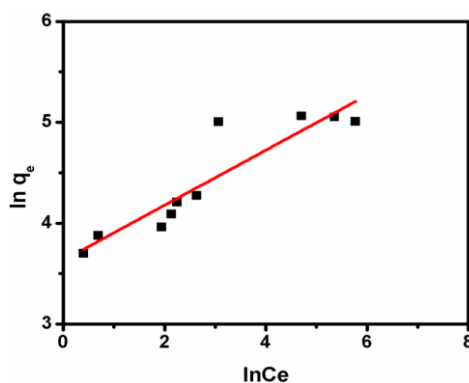


Fig. 11 Freundlich isotherm plot for the adsorption of Pb(II) ions onto NiO nanoparticles (adsorbent dosage 0.06 g, contact time 30 min; pH=6, temperature 293 K)

Table. 2 Adsorption isotherm model parameters of adsorption of Pb(II) on NiO nanoparticles at pH=6 and 293 K

Isotherm Model	Parameters
Langmuir Isotherm	
q_m (mg/g)	166
K_L (L/mg)	0.1136
R^2	0.9957
Freundlich isotherm	
K_F (mg/g)	37.788
n	3.676
R^2	0.8259

Adsorption kinetics

In order to investigate the rate adsorption of Pb (II) ions on NiO nanoparticles, the experimental data are analyzed using a number of kinetic models such as pseudo-first-order, pseudo-second-order, and intra-particle diffusion models.

Pseudo-first-order model

The pseudo-first-order rate expression, also known as the Lagergren equation, is generally expressed by the following equation [36]:

$$\ln(q_e - q_t) = \ln q_e - k_1 t \quad (10)$$

Where, q_e and q_t are the amounts of Pb (II) ions adsorbed on the surface of NiO at equilibrium (mg/g) and at any time t (mg/g), respectively and k_1 is pseudo-first order rate constant (/min). The values of k_1 and q_e can be determined from the slope and intercept of the linear plot of $\ln(q_e - q_t)$ versus t (Figure 12).

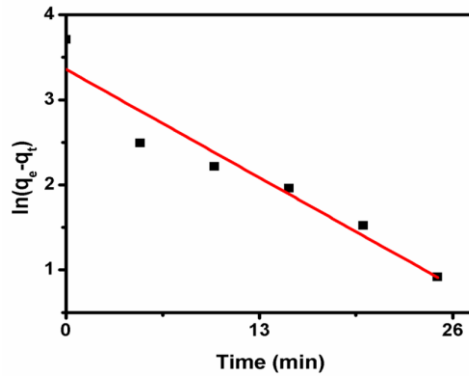


Fig. 12 The pseudo-first order plot for the adsorption of Pb (II) on NiO

Pseudo-second-order rate model

The pseudo-second order model is generally expressed as follows [36];

$$\frac{t}{q_t} = \frac{1}{k_2 q_e^2} + \frac{1}{q_e} t \quad (11)$$

Where, k_2 is the rate constant of adsorption, (g/mg/min).

The initial sorption rate (h), as $t \rightarrow 0$ is expressed as;

$$h = k_2 q_e^2 \quad (12)$$

Therefore, the initial sorption rate, h , the equilibrium sorption capacity, q_e , and the pseudo-second-order rate constant, k_2 , can be calculated experimentally from the slope and intercept of a plot of t/q_t versus t , as shown in Figure 13.

The resulted kinetic parameters evaluated for adsorption of Pb(II) ions on NiO nanoparticles are listed in Table 3. From the obtained results it is inferred that experimental results better agreed with pseudo-second-order model instead of pseudo-first-order model. The linearity constant for pseudo-second-order is 0.9886 which is close to unity. In addition, the experimental q_e value (45.45 mg/g) is very close to the theoretical value of q_e (40.83 mg/g) obtained from pseudo-second-order model, confirming the validity of that model to the adsorption of Pb (II) ions on NiO. The validation of the pseudo-second order kinetic model suggested that the adsorption of the Pb (II) ions on NiO occurred via chemisorption mechanism through electrostatic attractions between sorbent and sorbate [38, 39].

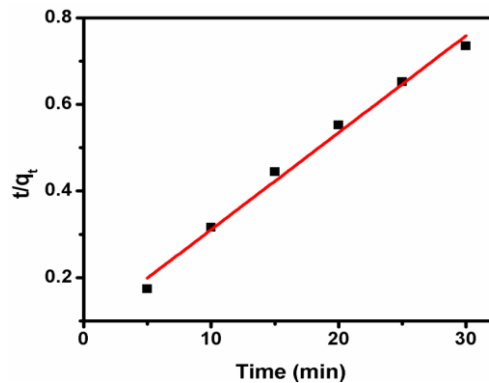


Fig. 13 The pseudo-second order plot for the adsorption of Pb (II) on NiO

Table. 3 Kinetic parameters for adsorption of Pb (II) ions on NiO nanoparticles

Kinetic Equation	Parameters
$q_e(\text{theor})$	40.83
Pseudo-First Order	
k_1 (/min)	0.0979
q_e (cal) (mg/g)	28.76
R^2	0.9134
Pseudo-Second Order	
k_2 (g/mg/min)	0.0056
q_e (cal) (mg/g)	45.45
h	11.5679
R^2	0.9886
Intra-Particle Diffusion	
k_{id} (mg/g/min ^{0.5})	6.954
R^2	0.8750

Intra-Particle Diffusion Model

The intra-particle diffusion model, proposed by Weber and Morris, is employed in adsorption kinetics to determine rate limiting step. It is expressed as [37]:

$$q_t = k_{id}\sqrt{t} + C \quad (13)$$

Where, k_{id} (mg/g/min^{1/2}) is the intra-particle diffusion rate constant and C is the intercept related to the film thickness.

Adsorption mechanism mainly proceed via film diffusion (mass transfer through surface of the adsorbent) followed by intra-particle diffusion (mass transfer from surface into pores of adsorbent) [40, 41]. In a batch process possibility of intra-particle diffusion is higher in contrast to film diffusion. If intra-particle diffusion is involved in sorption process then the plot of q_t against square root of t would be a straight line passing through the origin.

Figure 14 shows that straight line does not pass through the origin for the adsorption process of Pb (II) on NiO nanoparticles. The deviation of the straight line from the origin, as shown in figure, clearly indicates that the film diffusion is a rate determining step instead of intra-particle diffusion for the adsorption process [42]. Further the value of linearity constant is very low as 0.8750 thus confirming that intra-particle diffusion is not followed.

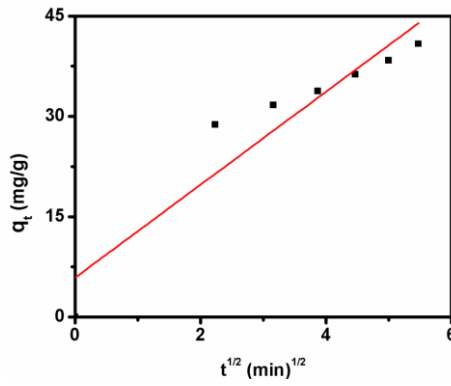


Fig. 14 Intra-particle diffusion plot for the adsorption of Pb (II) on NiO

Adsorption thermodynamics

Energy changes during adsorption process is demonstrated by evaluating thermodynamic parameters such as Gibbs energy changes (ΔG°), enthalpy changes (ΔH°), and entropy changes (ΔS°). Thermodynamics parameters are calculated by using the following expressions [43]:

$$\Delta G^\circ = -RT \ln K_C \quad (14)$$

$$K_d = \frac{C_{As}}{C_e} \quad (15)$$

$$\ln K_D = \frac{\Delta S^\circ}{R} - \frac{\Delta H^\circ}{RT} \quad (16)$$

Where, R is gas constant (8.314 J/K mol), C_{As} is the solid phase concentration at equilibrium (mg/L), k_d is equilibrium constant and T is absolute temperature (K). ΔH° and ΔS° can be calculated from the slope and intercept of the plot of $\ln k_d$ against $1/T$ (Figure 15).

The calculated values for ΔG° , ΔH° , and ΔS° are shown in Table 4. The positive value of ΔH° indicates that the adsorption of Pb (II) ions on NiO is endothermic in nature. The positive value of ΔS° reflects that the process of adsorption is spontaneous, and thermodynamically possible. The positive value of ΔS° also demonstrated some interactions at liquid/solid interface. The negative values of ΔG° suggest spontaneity and feasibility of the adsorption process at higher temperature.

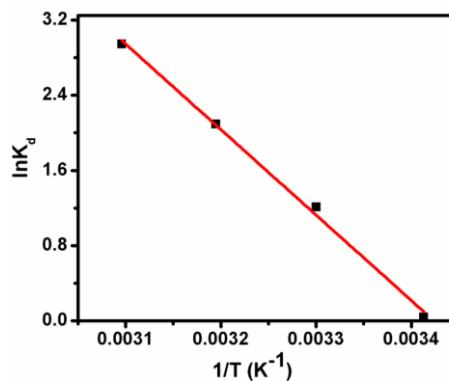


Fig. 15 Adsorption thermodynamics for Pb (II) adsorption on NiO

Table. 4 Thermodynamics parameters for adsorption of Pb (II) on NiO

Temperature (K)	ΔG° (kJ/mol)	ΔH° (kJ/mol)	ΔS° (J/K mol)
293	-2.53543	75.61	0.258
303	-8.43365		
313	-21.0548		
323	-51.023		

4. Conclusion

In this study, NiO nanoparticles are synthesized via novel sonochemical method and their effectiveness is verified by employing them as adsorbent for eradication of Pb (II) ions from water. Batch process is applied to study numerous operational parameters like adsorbent dose, solution pH, contact time, initial metal ion concentration, and temperature. Langmuir and Freundlich isotherms are used to fit experimental equilibrium data, though the Langmuir isotherm model fitted better with high regression co-efficient. Based on Langmuir isotherms, the maximum monolayer adsorption capacity for Pb (II) ions are calculated as 166 mg/g. Adsorption process revealed that the initial metal ion uptake is rapid and equilibrium is achieved within 30 min. Experimental results indicated that the adsorption process obeys pseudo-second-order reaction kinetics model. Based on the intra-particle diffusion model, it can be concluded that the adsorption process exhibits boundary layer diffusion. Thermodynamics parameters revealed that the adsorption process is endothermic as well as spontaneous in nature. Based on the obtained adsorption capacity, NiO nanoparticles can be used to treat water containing heavy metal ions.

References

- [1] F. Ji, C. Li, B. Tang, J. Xu, G. Lu, P. Liu, *Chem Eng J* **209**, 325 (2012).
- [2] T. Madrakian, A. Afkhami, B. Zadbou, M. Ahmadi, *J Ind Eng Chem* **21**, 1160 (2015).
- [3] S. H. Jang, B. G. Min, Y. G. Jeong, W. S. Lyoo, S. C. Lee, *J Hazard Mater* **152**, 1285 (2008).
- [4] L. Xiong, C. Chen, Q. Chen, J. Ni, *J Hazard Mater* **189**, 741(2011).
- [5] A. Özverdi, M. Erdem, *J Hazard Mater* **137**, 626 (2006).
- [6] S. Mustafa, S. Tasleem, A. Naeem, M. Safdar, *Colloids Surf., A* **330**, 8 (2008).
- [7] Z. M. Khoshhesab, Z. Hooshyar, M. Sarfaraz. *Synth React Inorg Met-Org Chem* **41**, 1046 (2011).
- [8] C. Luo, J. Wang, P. Jia, Y. Liu, J. An, B. Cao, K. Pan, *Chem Eng J* **262**, 775 (2015).
- [9] R. M. Moattari, S. Rahimi, L. Rajabi, A. A. Derakhshan, M. Keyhani M, *J Hazard Mater* **283**, 276 (2015).
- [10] S. R. Popuri, Y. Vijaya, V. M. Boddu, K. Abburi, *Bioresour Technol* **100**, 194 (2009).
- [11] S. Luo, X. Xu, G. Zhou, C. Liu, Y. Tang, Y. Liu, *J Hazard Mater* **274**, 145 (2014).
- [12] Q. Ou, L. Zhou, S. Zhao, H. Geng, J. Hao, Y. Xu, H. Chen, X. Chen, *Chem Eng J* **180**, 121(2012).
- [13] D. Mohammadyani, S. Hosseini, S. Sadrnezhaad, Sonochemical Synthesis of Nickel Oxide Nano-particle.
- [14] A. Barakat, M. Al-Noaimi, M. Suleiman, A. S. Aldwayyan, B. Hammouti, T. B. Hadda, S. F. Haddad, A. Boushala, I. Warad, *Int J Mol Sci* **14**, 23941 (2013).
- [15] X. Li, X. Zhang, Z. Li, Y. Qian, *Solid State Commun* **137**, 581 (2006).
- [16] A. G. Al-Sehemi, A. S. Al-Shihri, A. Kalam, G. Du, T. Ahmad, *J Mol Struct* **1058**, 56 (2014).
- [17] K. Anandan, V. Rajendran, *Mater Sci Semicond Process* **14**, 43 (2011).
- [18] R. Ahmad, *J Hazard Mater* **171**, 767 (2009).
- [19] O. Aksakal, H. Uzun, *J Hazard Mater* **181**, 666 (2010).

- [20] G. Crini, H. N. Peindy, F. Gimbert, C. Robert, *Sep Purif Technol* **53**, 97 (2007).
- [21] O. Amuda, A. Giwa, I. Bello, *Biochem Eng J* **36**, 174 (2007).
- [22] D. A. Dzombak, F. M. Morel, *Surface complexation modeling: hydrous ferric oxide*, John Wiley & Sons, New York, (1990).
- [23] Y-X. Zhang, X-Y. Yu, Z. Jin, Y. Jia, W-H. Xu, T. Luo, B-J. Zhu, J-H. Liu, X-J. Huang, *J Mater Chem* **21**, 16550 (2011).
- [24] S. İnan, Y. Altaş, *Sep Sci Technol* **45**, 269 (2010).
- [25] T. Sheela, Y. A. Nayaka, *Chem Eng J* **191**, 123 (2012).
- [26] A. Farghali, M. Bahgat, A. E. Allah, M. Khedr, *BJBAS* **2**, 61 (2013).
- [27] Y. Tian, C. Ji, M. Zhao, M. Xu, Y. Zhang, R. Wang, *Chem Eng J* **165**, 474 (2010).
- [28] M. Xu, Y. Zhang, Z. Zhang, Y. Shen, M. Zhao, G. Pan, *Chem Eng J* **168**, 737 (2011).
- [29] A-H. Chen, C-Y. Yang, C-Y. Chen, C-Y. Chen, C-W. Chen, *J Hazard Mater* **163**, 1068 (2009).
- [30] I. Langmuir, *SOLIDS JACS* **38**, 2221 (1916).
- [31] M. Özacar, İ. A. Şengil, H. Türkmenler, *Chem Eng J* **143**, 32 (2008).
- [32] G. Mckay, H. Blair, J. Gardner, *J Appl Polym Sci* **27**, 3043 (1982).
- [33] H. Freundlich, W. Heller, *JACS* **61**, 2228 (1939).
- [34] M. F. Sawalha, J. R. Peralta-Videa, J. Romero-Gonzalez, M. Duarte-Gardea, J. L. Gardea-Torresdey, *J Chem Thermodyn* **39**, 488 (2007).
- [35] S. Azizian, *J Colloid Interface Sci* **276**, 47 (2004).
- [36] W. J. Weber, J. C. Morris, *Journal of the Sanitary Engineering Division* **89**, 31 (1963).
- [37] F. Keyhanian, S. Shariati, M. Faraji, M. Hesabi, *ARAB J CHEM* (in press) (2011).
- [38] J. Song, H. Kong, J. Jang, *J Colloid Interface Sci* **359**, 505 (2011).
- [39] M. Ramakrishnan, S. Nagarajan, *Acta Chim. Slov* **56**, 282 (2009).
- [40] G. Boyd, A. Adamson, Jr. L. Myers, *JACS* **69**, 2836 (1947).
- [41] Q-S. Liu, T. Zheng, P. Wang, J-P. Jiang, N. Li, *Chem Eng J* **157**, 348 (2010).
- [42] T-t. Li, Y-g. Liu, Q-q. Peng, X-j. Hu, T. Liao, H. Wang, M. Lu, *Chem Eng J* **214**, 189 (2013).